Radiofrequency ablation of lung tumors using a multitined expandable electrode: impact of the electrode's array diameter on local tumor progression

ABSTRACT

Purpose: To retrospectively investigate the impact of the electrode's array diameter on local tumor progression after lung radiofrequency ablation.

Materials and Methods: This study included 651 lung tumors treated using multitined expandable electrodes and followed up for ≥6 months. The mean long-axis tumor diameter was 12 ± 7 mm (range, 2–42 mm). The difference between the electrode's array diameter and tumor diameter (DAT) was used to investigate the impact of the electrode's array diameter. All tumors were classified into 2 groups according to various variables including DAT (≥10 mm or <10 mm). The primary technique efficacy rates were calculated using Kaplan-Meier analysis and compared between the 2 groups of each variable using the log-rank test. In addition, crude and multivariate multilevel survival analyses were performed by sequentially including DAT and the other variables in 5 models.

Results: The median DAT for the 651 tumors was 12 mm (range -15–24 mm).

The technique efficacy rate was significantly lower in the <10-mm DAT group than in the ≥10-mm group ($P < 0.001$). In the crude and multivariate multilevel survival analyses, <10-mm DAT was a significant risk factor for local progression in all models, except model 5 ($P = 0.067$). In the ≥10-mm group, the technique efficacy rates were not significantly different between the two ≥10-mm DAT sub-groups (10 to <15-mm DAT vs. ≥15-mm DAT).

Conclusion: DAT is an important risk factor for local progression, and we recommend an electrode that is ≥10 mm larger than the tumor diameter.

INTRODUCTION

Since the first report of radiofrequency (RF) ablation of lung tumors in 2000 (1), various risk factors for local progression have been reported (2–6). We previously reported that multitined expandable electrodes are significantly more efficacious than internally cooled electrodes, based on the results of multivariate multilevel analysis (2).

The technical goal of RF ablation is to obtain an adequate ablative margin (7). In lung tumors, ground-glass opacity around the treated tumors is often observed immediately after RF ablation (8,9). A >5-mm circumferential ground-glass opacity margin is reportedly the minimum margin required to ensure complete tumor ablation (10). However, because post-ablation ground-glass opacity shows not only coagulation necrosis but also parenchymal hemorrhage, congestion, and sublethal thermal damage (11,12), it might be difficult to accurately demarcate the ablation zone from non-ablation related opacities.

It is essential to use an electrode with an adequately large array diameter and/or to use several overlapping ablations to achieve the desired ablation margin. Larger tumors usually require multiple overlapping ablations. However, overlapping ablation is reportedly not a simple procedure (13–15). The size of the

composite thermal injury created by overlapping multiple thermal ablation spheres is surprisingly small relative to the number of ablations performed, based on a computer analysis (15).

Therefore, the purpose of this study was to retrospectively evaluate the impact of the electrode's array diameter on local tumor progression after lung RF ablation.

MATERIALS AND METHODS

Our institutional review board approved this retrospective study and waived the need for informed consent to use the patients' medical data.

Study population

Between June 2001 and August 2011, we performed RF ablation of 1326 lung tumors in 488 patients using multitined expandable electrodes (LeVeen; Boston Scientific, Natick, MA) or internally cooled electrodes (Cool-tip; Valleylab, Boulder, CO). Of these, the following tumors were excluded: 437 tumors (163 patients) treated using the internally cooled electrodes, 234 tumors

(71 patients) with a follow-up period <6 months, and 4 tumors (3 patients) due to RF ablation followed by scheduled radiotherapy without local progression. Consequently, 651 lung tumors (595 metastatic lung tumors and 56 primary lung tumors) in 251 patients (150 men and 101 women; mean age, 65 ± 12 years; age range, 24–94 years) were included (Fig. 1). The study cohort included 179 patients (505 tumors) who have been described previously (2,16–19); their follow-up data were updated for the present study.

The mean long-axis tumor diameter was 12 ± 7 mm (range, 2–42 mm). The nature and number of the tumors are summarized in Table 1. The diagnosis was mainly based on the results of serial computed tomography (CT). In primary lung tumors, 53 of 56 (95%) were histologically confirmed. The median number of ablated tumors per patient was 2 (range, 1–18); 123 patients had a solitary tumor, and 128 patients had multiple tumors (29 had >5 tumors). The number of overlapping ablations was 1 in 167 tumors, 2 in 362 tumors, 3 in 85 tumors, 4 in 23 tumors, and ≥5 in 14 tumors. Adjuvant systemic therapy was administered for 121 patients after the initial RF ablation: chemotherapy (n = 111), immunotherapy (n = 8), hormone therapy (n = 1), or hormone therapy followed by chemotherapy (n = 1). In the remainder of the patients, the use of systemic therapy was not

described in the patient charts.

Radiofrequency ablation techniques

The details of the procedure have been described previously (16). Briefly, RF ablation was always performed percutaneously using CT fluoroscopy (Asteion, Toshiba, Otawara, Japan; Aquilion 16, Toshiba, Otawara, Japan; and Aquilion CX, Toshiba, Otawara, Japan) by interventional radiologists with 7–11 years of experience with CT fluoroscopy-guided radiofrequency ablation of lung tumors. The electrodes that were used for the 651 tumors included a multitined expandable electrode with an array diameter of 2 cm (n = 462), 3 cm (n = 155), 3.5 cm (n = 25), or 4 cm (n = 9). Before December 2006, the array diameter primarily depended on the location and size of the tumor as well as the physician's preference. Then, our ablation strategy changed to use an electrode with an array diameter ≥10 mm larger than the tumor diameter, when possible. We treated 339 tumors during the first six years (2001–2006) and 312 tumors during the later years (2007–2011).

The electrode was introduced into the tumor and connected to an RF generator (RF 2000 or RF 3000; Boston Scientific, Natick, MA). Until April 2005,

the RF 2000 (maximum power output, 90 W) was used; then, the RF 3000 (maximum power output, 200 W) was used. RF energy was applied until there was a rapid increase in the impedance or until automatic shut-off occurred at 15 minutes; this was repeated twice at each site. The mean maximum RF generator power output was 52 ± 36 W, and the mean total ablation time was 20 ± 14 minutes.

Regardless of the tumor characteristics, every procedure aimed to ablate the tumor with a ≥5 mm margin of parenchyma, which is observed as ground-glass opacity around the tumor. If the tumor was not surrounded by ≥5 mm of ground-glass opacity immediately after the ablation, the ablation was repeated after repositioning of the electrode. The typical ablation was performed at 2 sites (the peripheral and hilar parts of the tumor) to create a spherical ablation zone, because a single ablation zone is typically an oblate spheroid shape (Fig. 2). If the tumors were surrounded by ≥5 mm ground-glass opacity after ablation with a single electrode position, additional ablations were not performed.

Follow-up and assessment of local progression

Patient charts were retrospectively reviewed, with no prior knowledge

regarding the outcome of the RF ablation of each tumor.

The follow-up protocol included chest CT scans at 1, 3, 6, 9, and 12 months after the procedure and at 6-month intervals thereafter. Unless contraindicated, contrast enhancement was performed to assess the outcomes of RF ablation at each follow-up examination. Positron emission tomography (PET) was also performed as an adjunct for the diagnosis of local progression.

The assessment of local progression has been described previously (16). Local tumor progression is considered to have occurred when the ablation zone is circumferentially enlarged or when an irregular, scattered, nodular, or eccentric focus appears in the ablation zone. This focus typically exhibits some degree of contrast enhancement (i.e., enhancement >15 HU) and is thus distinguished from the unenhanced necrotic tumor tissue (20). A new pulmonary metastasis is deemed to occur when a new nodule is observed outside of the ablated zone. The decision regarding local progression was based on the review of the patient charts. When the radiology report differed from the attending physician's diagnosis, a third investigator made the final decision.

Investigation of various factors, including DAT

To investigate the impact of the electrode's array diameter on local tumor progression, we used the difference between the electrode's array diameter and long-axis tumor diameter (DAT). DAT is calculated using the following formula: electrode’s array diameter − long-axis tumor diameter (Fig. 3). The other recorded variables were a procedure-related factor (number of overlapping ablations), patient-related factors (sex, age, pulmonary emphysema), tumor-related biological factors (primary or metastatic, sarcoma or carcinoma), and tumor-related physical factors (long-axis diameter, location, contact with a blood vessel, contact with a bronchus). Although treatment period (2001–2006 or 2007–2011) could be a potential risk factor, it was not included in the analysis because it was strongly related to DAT.

If the center of the tumor was located in the inner or outer half of the lungs on the axial CT images obtained before RF ablation, the tumor location was considered as central or peripheral, respectively. The tumor was considered to be in contact with a blood vessel if it was contiguous to a vessel ≥3 mm in diameter. Similarly, the tumor was considered to be in contact with a bronchus when it was contiguous to a bronchus ≥2 mm in inner diameter.

Statistical analysis

The following continuous variables were dichotomized for analysis: DAT (<10 or ≥10 mm), age (<60 or ≥60 years), long-axis tumor diameter (<20 or ≥20 mm), and number of overlapping ablations (≤2 or ≥3).

Student's *t*-tests were used to compare the differences in DAT between the treatment periods (2001–2006 vs. 2007–2011) as well as the differences in the number of overlapping ablations between DAT (<10 vs. ≥10 mm).

The technique efficacy rate is defined as the percentage of target tumors successfully eradicated following the initial procedure (7). The technique efficacy rates were calculated using Kaplan-Meier analysis and compared between the 2 groups of each variable with the log-rank test. Then, to adjust for potential confounders, we estimated hazard ratios (HRs) and 95% confidence intervals (CIs) for local progression using multilevel mixed effects parametric survival analysis with a random intercept term. Our data consisted of hierarchical data composed of patients, with tumors nested within each patient; we set level 1 as tumors and level 2 as patients. We sequentially included various factors in five models. After conducting a crude model (model 1, including DAT only), we adjusted for patient-related factors (model 2). Then, we additionally adjusted for

the procedure-related factor (model 3), tumor-related biological factors (model 4), and tumor-related physical factors (model 5).

Then, we also calculated the technique efficacy rates for two ≥10-mm DAT groups (10 to <15 mm and ≥15 mm), and the rates were also compared between these 2 groups using univariate analysis with the log-rank test.

For all analyses, a *P* value < 0.05 was considered statistically significant. In the crude and multivariate multilevel survival analyses, HRs >1.00 indicated an increased risk for local progression. Student's *t*-tests, Kaplan-Meier analyses, and log-rank tests were performed using SPSS version 22 (IBM Corp., Armonk, NY, USA). Multilevel survival analyses were conducted using Stata version 13 (Stata Corp., College Station, TX, USA) (21).

RESULTS

The median DAT was 12 mm (mean, 11 ± 6 mm; range, -15–24 mm), while the mean DAT for the first 6 years and later years were 9 ± 6 mm and 14 ± 4 mm, respectively ($P < 0.001$). The mean numbers of overlapping ablations for the ≥10-mm DAT and <10-mm DAT groups were 1.8 ± 0.7 and 2.4 ± 1.3, respectively ($P < 0.001$). During the follow-up period (median, 21.0 months;

range, 6.0–91.6 months), local progression was observed in 67 (10.3%) tumors at 1.2–46.8 months (median, 10.1 months) after the initial RF ablation session. The overall technique efficacy rate was 93% (95% CI, 91–95%) at 1 year, 89% at 2 years (95% CI, 86–91%), and 86% (95% CI, 83–90%) at 3 years.

In the univariate analysis, the technique efficacy rate was significantly lower for the <10-mm DAT group than the ≥10-mm DAT group ($P < 0.001$) (Fig. 4). Significantly lower technique efficacy rates were also observed for ≥3 overlapping ablations ($P < 0.001$), primary lung tumors ($P < 0.001$), tumors with ≥20 mm long-axis diameter ($P < 0.001$), contact with a blood vessel ($P < 0.001$), and contact with a bronchus ($P < 0.001$) (Table 2). The results of the crude and multivariate multilevel survival analyses for the 651 tumors are shown in Table 3, and <10-mm DAT was significant in model 1 (HR, 3.21; 95% CI, 1.84–5.59; $P < 0.001$), model 2 (HR, 3.19; 95% CI, 1.83–5.56; $P < 0.001$), model 3 (HR, 2.70; 95% CI, 1.49–4.89; $P = 0.001$), and model 4 (HR, 2.39; 95% CI, 1.29–4.40; $P = 0.005$), but not model 5 (HR, 1.84; 95% CI, 0.96–3.55; $P = 0.067$). A primary lung tumor was statistically significant in models 4 and 5. None of the other variables were statistically significant.

In the ≥10-mm DAT group, 267 tumors were treated with 10 mm to <15

mm DAT, and 179 tumors were treated with ≥15 mm DAT. The technique efficacy rates were not significantly different between 10 mm to <15 mm DAT and ≥15 mm DAT ($P = 0.637$) (Fig. 5).

Of the 57 patients that died after the initial RF ablation (median, 25.4 months; range, 7.1–55.6 months), 44 died due to tumor progression.

DISCUSSION

DAT was a significant risk factor for local progression in the univariate analyses. Moreover, in the multivariate multilevel survival analysis, DAT was significant in all of the models except model 5. Therefore, we believe <10-mm DAT to be an important risk factor for local progression. In addition, a significant difference was not observed between the two ≥10-mm DAT sub-groups (10 to <15-mm DAT vs. ≥15-mm DAT) ($P = 0.637$). A large DAT might improve the technique efficacy rate. However, the adequate DAT value remains unclear.

A number of studies (2–6) have retrospectively or prospectively reported the local efficacy and risk factors for local progression with lung RF ablation. Although DAT was not included in any of these analyses, the study by de Baère et al. (3) might have indirectly demonstrated the effect of DAT with multitined

expandable electrodes that were ≥15 mm larger than the largest tumor diameter, when possible. Their technique efficacy rate was 93% at 18 months, which is better than other reported technique efficacy rates, even those reported by Okuma et al. (6) using only multitined expandable electrodes (61% at 1 year and 57% at 2 years).

The number of overlapping ablations in the <10-mm DAT group was significantly greater than that in the ≥10-mm DAT group ($P < 0.001$), indicating that RF ablation with a smaller DAT requires additional ablations after repositioning the electrode to obtain ≥5 mm ground-glass opacity around the target tumor. This could explain the technical complexity associated with the procedure. In addition, the electrode repositioning might cause unpredictable tumor cell displacement and impact the technique efficacy.

A primary lung tumor was statistically significant in the multivariate multilevel survival analyses models 4 and 5. In a previous assessment of the microscopic extension in primary lung cancer, 20% of adenocarcinomas and 9% of squamous cell carcinomas showed microscopic extension >5 mm from the main tumor (22). In addition, the surgical safety margin in segmentectomy for small primary lung tumors (≤20 mm) is reportedly 20 mm from primary lung

tumors (23). Therefore, a DAT ≥10 mm might not be sufficient for primary lung tumors. However, the differences between primary and metastatic tumors was not the primary focus of the present study; furthermore, statistical significance was only observed in models 4 and 5, which indicates the findings might not be robust.

Although previous multivariate analyses have identified tumor size as an independent factor for local progression (2,5,6), tumor size was the only risk factor in the univariate analysis, but not in the multivariate multilevel survival analysis in the present study. One reason might be the very small mean tumor size (12 ± 7 mm), with only 78 of the 651 (12.0%) tumors ≥20 mm. Therefore, tumor size may have limited effect on local progression.

This study had several limitations. First, the study was retrospective and conducted in a single institution, with a median follow-up period of 21 months, which might not have been long enough to detect local tumor progression, especially with slowly growing tumors. Second, the heterogeneity of the tumor characteristics and ablation techniques might have influenced the generalizability of the results. Third, the mean tumor diameter was small (12 ± 7 mm). Fourth, we did not evaluate the learning effect because of the change in treatment strategy. Fifth, we did not include systemic therapy in the analyses because various types of

tumors and anti-cancer drugs were included, and the impact of systemic therapy on local control varies. Last, the impact of local progression on patient survival was not investigated.

In conclusion, DAT is an important risk factor for local progression after RF ablation of lung tumors. We recommend the use of multitined expandable electrodes that are ≥10 mm larger than the tumor diameter, whenever possible.

REFERENCES

1. Dupuy DE, Zagoria RJ, Akerley W, Mayo-Smith WW, Kavanaugh PV, Safran H. Percutaneous radiofrequency ablation of malignancies in the lung. AJR Am J Roentgenol 2000; 174:57–59.

2. Hiraki T, Sakurai J, Tsuda T, et al. Risk factors for local progression after percutaneous radiofrequency ablation of lung tumors: evaluation based on a preliminary review of 342 tumors. Cancer 2006; 107:2873–2880.

3. de Baère T, Palussière J, Aupérin A, et al. Midterm local efficacy and survival after radiofrequency ablation of lung tumors with minimum follow-up of 1 year: prospective evaluation. Radiology 2006; 240:587–596.

4. Simon CJ, Dupuy DE, DiPetrillo TA, et al. Pulmonary radiofrequency ablation: long-term safety and efficacy in 153 patients. Radiology 2007; 243:268–275.

5. Gillams AR, Lees WR. Radiofrequency ablation of lung metastases: factors influencing success. Eur Radiol 2008; 18:672–677.

6. Okuma T, Matsuoka T, Yamamoto A, et al. Determinants of local progression after computed tomography-guided percutaneous radiofrequency ablation for unresectable lung tumors: 9-year experience in a single institution.

Cardiovasc Intervent Radiol 2010; 33:787–793.

7. Ahmed M, Solbiati L, Brace CL, et al. Image-guided tumor ablation: standardization of terminology and reporting criteria–a 10-year update. J Vasc Interv Radiol 2014; 25:1691–1705.
8. Bojarski JD, Dupuy DE, Mayo-Smith WW. CT imaging findings of pulmonary neoplasms after treatment with radiofrequency ablation: results in 32 tumors. AJR Am J Roentgenol 2005; 185:466–471.
9. Lee JM, Jin GY, Goldberg SN, et al. Percutaneous radiofrequency ablation for inoperable non-small cell lung cancer and metastases: preliminary report. Radiology 2004; 230:125–134.
10. Anderson EM, Lees WR, Gillams AR. Early indicators of treatment success after percutaneous radiofrequency of pulmonary tumors. Cardiovasc Intervent Radiol 2009; 32:478–483.
11. Yamamoto A, Nakamura K, Matsuoka T, et al. Radiofrequency ablation in a porcine lung model: correlation between CT and histopathologic findings. AJR Am J Roentgenol 2005; 185:1299–1306.
12. Goldberg SN, Gazelle GS, Compton CC, Mueller PR, McLoud TC. Radio-frequency tissue ablation of VX2 tumor nodules in the rabbit lung.

Acad Radiol 1996; 3:929–935.

13. Dodd GD 3rd, Soulen M, Kane R, et al. Minimally invasive treatment of malignant hepatic tumors: at the threshold of major breakthrough. Radiographics 2000; 20:9–27.
14. Rhim H, Goldberg SN, Dodd GD 3rd, et al. Essential techniques for successful radio-frequency thermal ablation of malignant hepatic tumors. Radiographics 2001; 21:S17–35; discussion S36-39.
15. Dodd GD 3rd, Frank MS, Aribandi M, Chopra S, Chintapalli KN. Radiofrequency thermal ablation: computer analysis of the size of the thermal injury created by overlapping ablations. AJR Am J Roentgenol 2001; 177:777–782.
16. Hiraki T, Gobara H, Mimura H, et al. Radiofrequency ablation of lung cancer at Okayama University Hospital: a review of 10 years of experience. Acta Med Okayama 2011; 65:287–297.
17. Matsui Y, Hiraki T, Gobara H, et al. Percutaneous radiofrequency ablation for pulmonary metastases from esophageal cancer: retrospective evaluation of 21 patients. J Vasc Interv Radiol 2014; 25:1566–1572.
18. Matsui Y, Hiraki T, Gobara H, et al. Long-term survival following

percutaneous radiofrequency ablation of colorectal lung metastases. J Vasc Interv Radiol 2015; 26:303–310.

19. Iguchi T, Hiraki T, Gobara H, et al. Radiofrequency ablation of lung metastases from adenoid cystic carcinoma of the head and neck: retrospective evaluation of nine patients. J Vasc Interv Radiol 2015; 26:703–708.
20. Abtin FG, Eradat J, Gutierrez AJ, Lee C, Fishbein MC, Suh RD. Radiofrequency ablation of lung tumors: imaging features of the postablation zone. Radiographics 2012; 32:947–969.
21. Crowther MJ. STMIXED: Stata module to fit multilevel mixed effects parametric survival models. Available at http://ideas.repec.org/c/boc/bocode/s457845.html. Accessed Feb 10, 2015.
22. Giraud P, Antoine M, Larrouy A, et al. Evaluation of microscopic tumor extension in non-small-cell lung cancer for three-dimensional conformal radiotherapy planning. Int J Radiat Oncol Biol Phys 2000; 48:1015–1024.
23. Swanson SJ. Segmentectomy for lung cancer. Semin Thorac Cardiovasc Surg 2010; 22:244–249.

Figure and Table Legends

Figure 1. Selection of patients for inclusion in the study

Figure 2. A 58-year-old man with metastasis from hepatocellular carcinoma: A multitined expandable electrode was placed at the peripheral (A) and hilar parts (B) of the tumor. CT image immediately after ablation (C) showed the target tumor with surrounding ground-glass opacity. (D) Schema of our typical ablation procedure to create a spherical ablation zone.

Figure 3. Schema showing the difference between the electrode's array diameter and long-axis tumor diameter (DAT)

Figure 4. Technique efficacy rate, compared between DAT ≥10 mm and DAT <10 mm

DAT, difference between the electrode's array diameter and long-axis tumor diameter

Figure 5. Technique efficacy rate, compared between ≥10-mm DAT subgroups

(10 to <15 mm and ≥15 mm)

The technique efficacy rates were not significantly different between the 2 groups ($P = 0.637$).

DAT, difference between the electrode's array diameter and long-axis tumor diameter

Table 1. Nature and number of lung tumors treated using radiofrequency ablation, by number of patients

Table 2. Univariate analyses using the log-rank test to determine the risk factors for local progression of lung tumors following radiofrequency ablation

Table 3. Crude and multivariate multilevel survival analyses to determine independent risk factors for local progression of lung tumors following radiofrequency ablation

Figure1

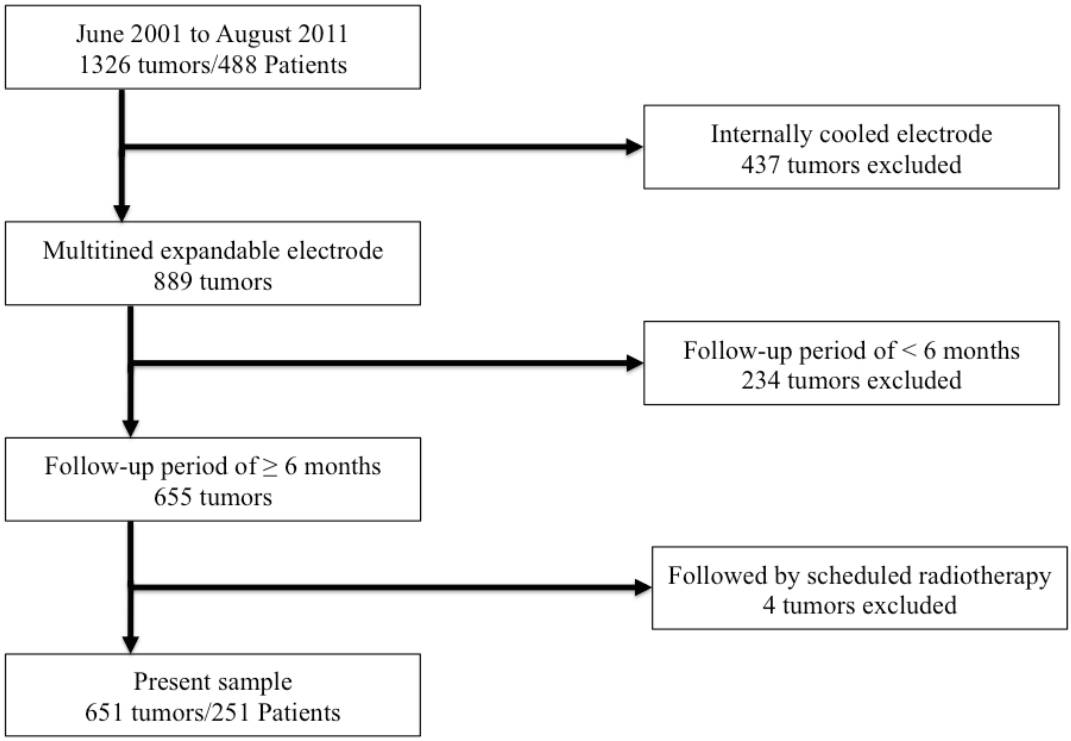
June 2001 to August 2011
1326 tumors/488 Patients
Internally cooled electrode
437 tumors excluded
Multitined expandable electrode
889 tumors
Follow-up period of < 6 months
234 tumors excluded
Follow-up period of ≥ 6 months
655 tumors
Followed by scheduled radiotherapy
4 tumors excluded
Present sample
651 tumors/251 Patients

Figure2A

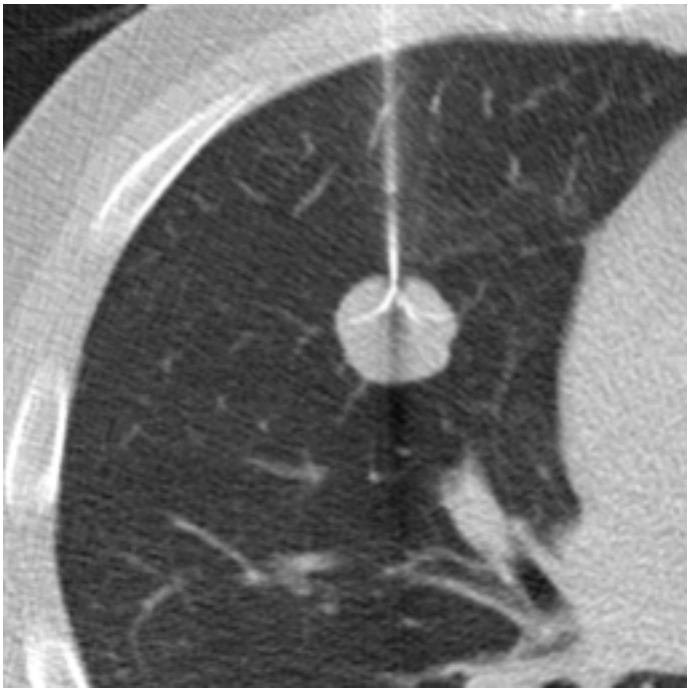

Figure2B

Figure2C

Figure2D

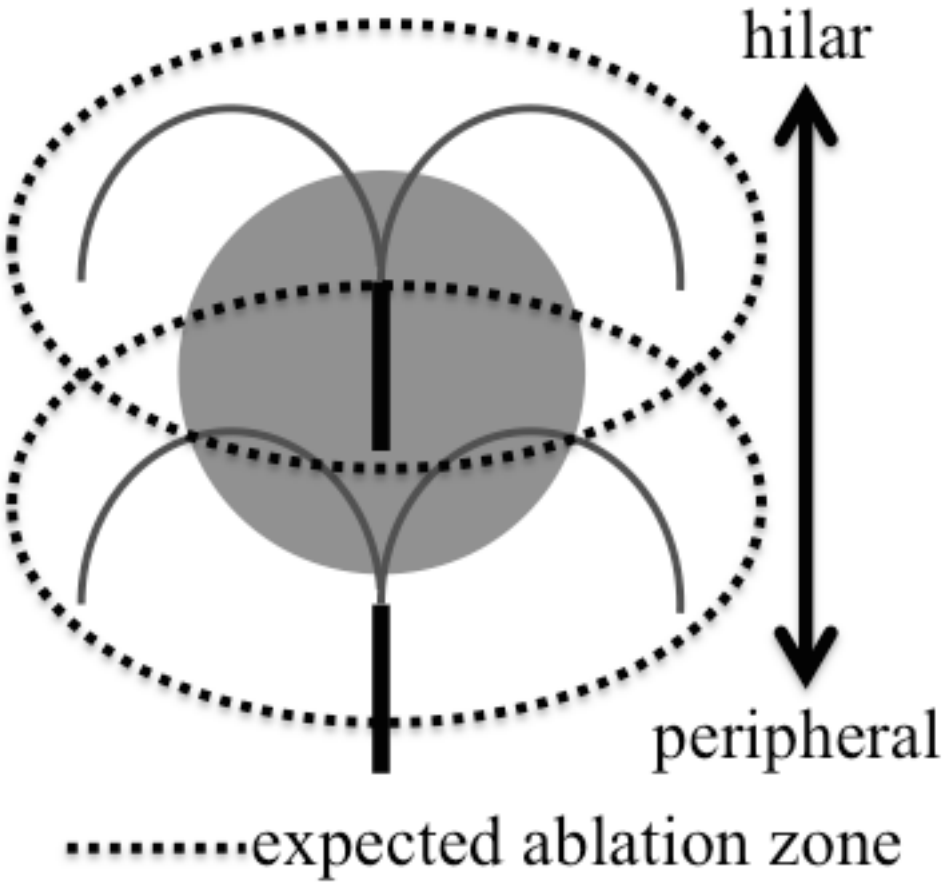

Figure3

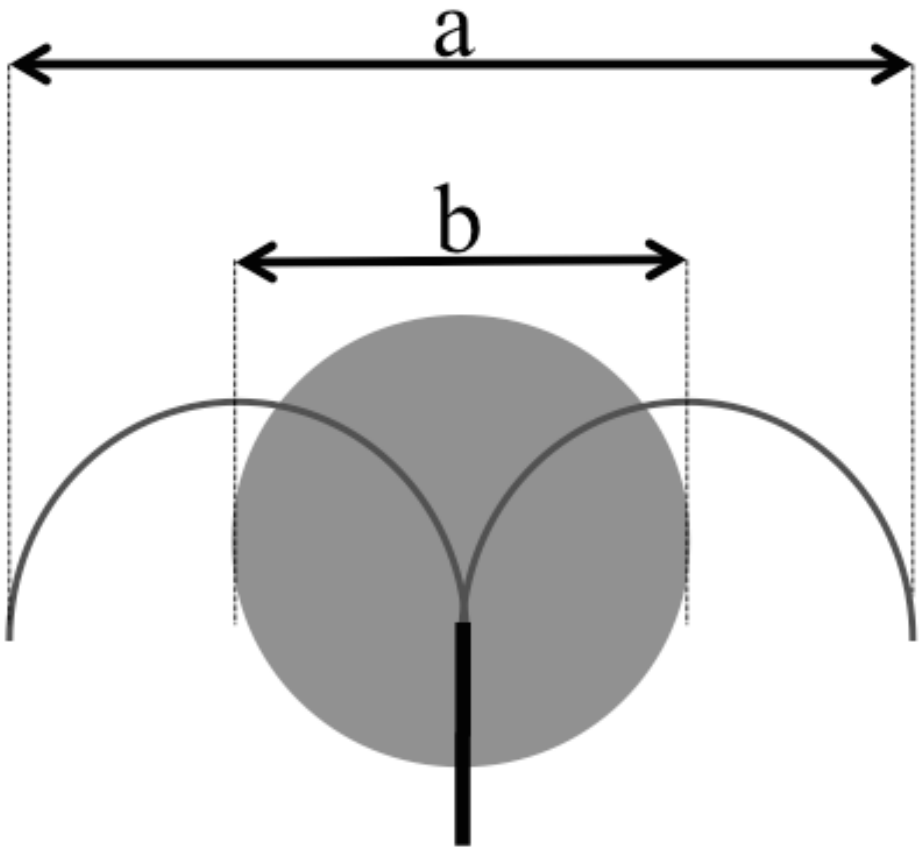

DAT = a – b (mm)

* a = the electrode's array diameter
b = long-axis tumor diameter

Figure4

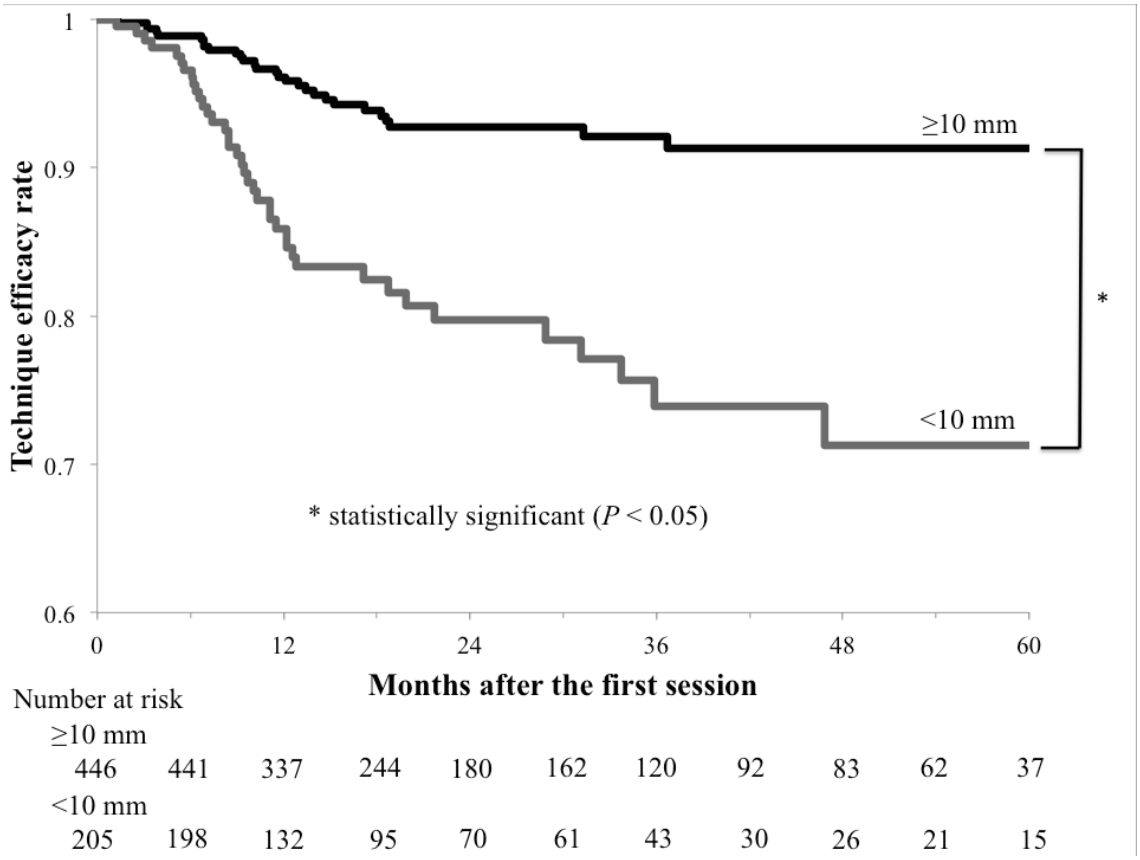
1
0.9
0.8
0.7
0.6
Technique efficacy rate
≥10 mm
<10 mm
*
* statistically significant (P < 0.05)
0
12
24
36
48
60
Months after the first session
Number at risk
≥10 mm
446 441 337 244 180 162 120 92 83 62 37
<10 mm
205 198 132 95 70 61 43 30 26 21 15

Figure5

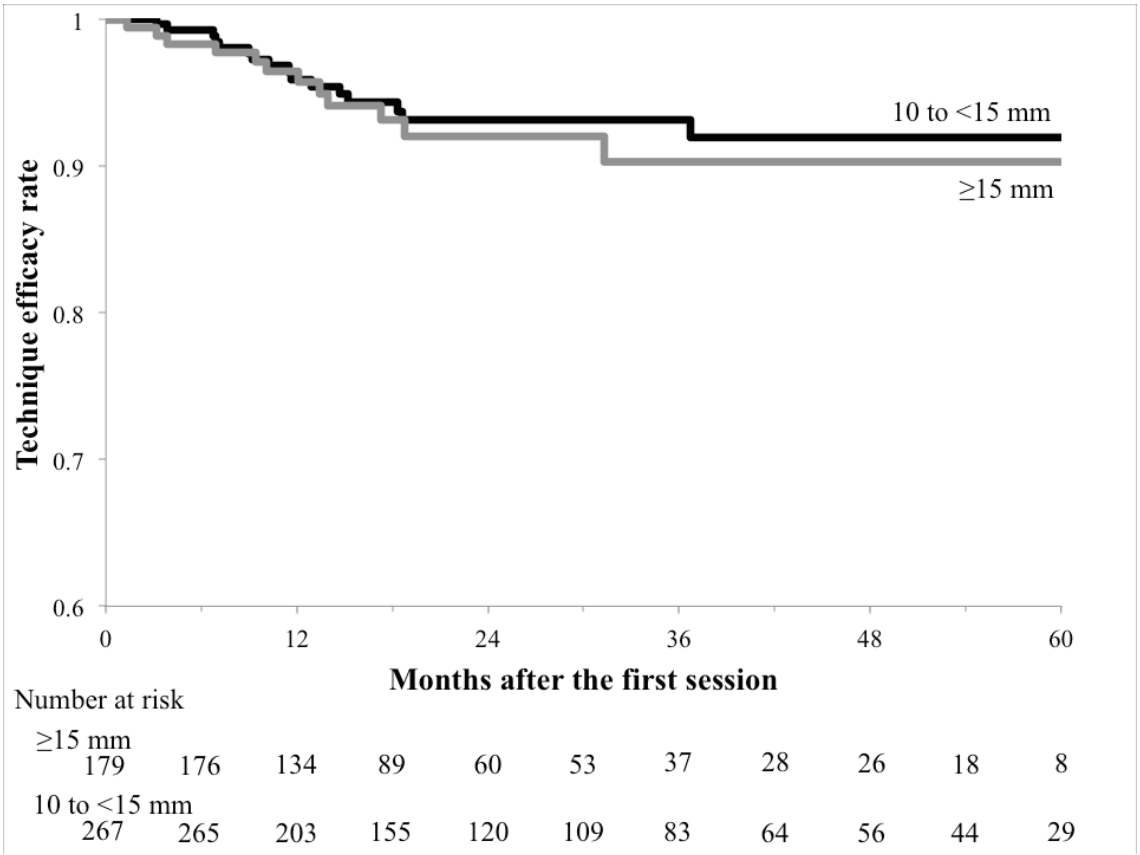
1
0.9
0.8
0.7
0.6
Technique efficacy rate
10 to <15 mm
≥15 mm
0
12
24
36
48
60
Months after the first session
Number at risk
≥15 mm
179 176 134 89 60 53 37 28 26 18 8
10 to <15 mm
267 265 203 155 120 109 83 64 56 44 29

Table1

Variable	Patients (n)	Tumors (n)
Type of tumor		
Primary lung tumor	51	56*
Metastatic lung tumor	200	595
Colorectal cancer	71	192
Lung cancer	24(29**)	49
Hepatocellular carcinoma	20	68
Renal cell carcinoma	14	58
Uterine sarcoma	12	30
Esophageal cancer	12	20
Bone and soft tissue tumors	9	19
Others	38	159
Number of treated tumors per patient		
1	123	
2	47	
3	25	
4	15	
5	12	
≥6	29	

*Five patients had double primary lung tumors.

**Five patients had both primary and metastatic lung tumors.

Table2

Variables		Number of tumors	Technique efficacy rate		*P*
			1 year (%)	2 year (%)	
Procedure-related factors					
DAT (mm)					< 0.001
	< 10	205	86	80	
	≥ 10	446	96	93	
Number of overlapping ablations					< 0.001
	≤ 2	529	95	91	
	≥ 3	122	86	79	
Patient-related factors					
Sex					0.324
	Men	415	92	87	
	Women	236	94	92	
Age (years)					0.812
	< 60	285	92	88	
	≥ 60	366	93	89	
Pulmonary emphysema					0.435
	Yes	98	91	85	
	No	553	93	89	
Tumor-related factors (Biological)					
Primary vs. Metastatic					< 0.001
	Primary	56	87	76	
	Metastatic	595	93	90	
Sarcoma vs. Carcinoma					0.824
	Sarcoma	49	93	86	
	Carcinoma	602	93	88	
Tumor-related factors (Physical)					
Long-axis diameter (mm)					< 0.001
	< 20	573	95	90	
	≥ 20	78	80	75	
Location					0.174
	Peripheral	513	93	89	
	Central	138	92	86	
Contact with a blood vessel					< 0.001
	Yes	151	88	80	
	No	500	94	91	
Contact with a bronchus					< 0.001
	Yes	78	83	71	
	No	573	94	91	

DAT, difference between the electrode's array diameter and long-axis tumor diameter

Table3

Fixed effect parameters	Model 1			Model 2			Model 3			Model 4			Model 5		
	HR	95%CI	*P*	HR	95%CI	*P*	HR	95%CI	*P*	HR	95%CI	*P*	HR	95%CI	*P*
DAT															
≥ 10 mm	1.00	reference		1.00	reference		1.00	reference		1.00	reference		1.00	reference	
< 10 mm	3.21	1.84 – 5.59	<0.001	3.19	1.83 – 5.56	<0.001	2.70	1.49 – 4.89	0.001	2.39	1.29 – 4.40	0.005	1.84	0.96 – 3.55	0.067
Patient-related factors															
Sex (Men vs. Women†)				1.20	0.60 – 2.40	0.611	1.20	0.59 – 2.43	0.611	1.47	0.69 – 3.11	0.314	1.40	0.67 – 2.94	0.373
Age (≥ 60 years vs. < 60 years†)				1.09	0.56 – 2.11	0.806	1.04	0.53 – 2.04	0.918	0.84	0.41 – 1.71	0.627	0.83	0.41 – 1.68	0.599
Pulmonary emphysema (Yes vs. No†)				1.13	0.49 – 2.59	0.774	1.15	0.50 – 2.68	0.742	0.89	0.36 – 2.19	0.808	0.91	0.38 – 2.21	0.838
Procedure-related factor															
Number of overlapping ablations (≥ 3 vs. ≤ 2†)							1.72	0.94 – 3.18	0.081	1.76	0.94 – 3.29	0.078	1.42	0.74 – 2.75	0.269
Tumor-related factors (Biological)															
Tumor type (Primary vs. Metastatic†)										2.77	1.17 – 6.53	0.020	2.58	1.09 – 6.07	0.031
Tumor type (Sarcoma vs. Carcinoma†)										1.48	0.38 – 5.74	0.568	1.49	0.39 – 5.70	0.558
Tumor-related factors (Physical)															
Long-axis diameter (≥ 20 mm vs. < 20 mm†)													1.67	0.80 – 3.49	0.169
Location (Central vs. Peripheral†)													1.18	0.59 – 2.33	0.641
Contact with a blood vessel (Yes vs. No†)													1.38	0.68 – 2.80	0.379
Contact with a bronchus (Yes vs. No†)													1.62	0.76 – 3.45	0.214
Random effect parameter	Var	95%CI		Var	95%CI		Var	95%CI		Var	95%CI		Var	95%CI	
between patient variance	1.36	0.60 – 3.13		1.35	0.58 – 3.13		1.43	0.63 – 3.26		1.48	0.66 – 3.32		1.36	0.59 – 3.13	

† reference category

DAT, difference between the electrode's array diameter and long-axis tumor diameter; HR, hazards ratio; CI, confidence interval